

# METHODOLOGY FOR POROSIMETRY IN VIRTUAL CEMENTITIOUS COMPOSITES TO ECONOMICALLY AND RELIABLY ESTIMATE PERMEABILITY

KAI LI<sup>✉</sup>, PIET STROEVEN AND NGHI LB LE

Faculty of Civil Engineering and Geosciences, Delft University of Technology, Stevinweg 1, 2628CN Delft, the Netherlands

e-mail: K.Li-1@tudelft.nl; P.Stroeven@tudelft.nl; L.B.N.Le@tudelft.nl

(Received January 12, 2015; revised May 21, 2015; accepted May 25, 2015)

## ABSTRACT

A novel methodology is described for porosimetry as well as for water transport through the pore system in dynamic DEM-based virtual cementitious materials. The pore network topology, the pore size distribution and the pore connectivity are assessed on the basis of a robotics-inspired pore delineation method and star volume measurements. Permeability estimates are based on a tube network model that incorporates these parameters and a shape factor. Since concrete contains in practical situations a variable amount of water, permeability estimation is presented as a function of the state of saturation. Satisfactory agreement is found with experimental data, validating the methodology. Earlier, the various “building blocks” were separately validated.

Keywords: DEM, permeability, porosimetry, water saturation.

## INTRODUCTION

Transport-based durability problems still constitute complicated issues in experimental researches. Water permeability testing of the real concrete (“realcrete”) is quite laborious, time-consuming and thus expensive. Speeding up the transport process introduces uncertainties as to the interpretation of obtained results. Therefore, the most common experimental approach in concrete technology is by MIP (Mercury Intrusion Porosimetry) (e.g., Abell *et al.*, 1999). The instrumentation is relatively cheap and as a consequence available in many research laboratories in the field of concrete technology. The experiments can be directly interpreted in terms of the three-dimensional (3D) pore size distribution (PoSD). Unfortunately, it has been demonstrated that a wide gap can exist between image analysis and MIP data, as Fig. 1 may prove (Diamond, 2000). Very narrow pathways in the pore system (so called “bottle necks”) prevent passage of the pressurized mercury making part of the pore network inaccessible. The surface layer of the concrete specimens can also lead to limited inaccessible of the mercury to the underlying part of the pore network structure. These are two widely accepted deficiencies of the approach giving rise to the biased PoSD information as compared to the image analysis results.

An incidentally used alternative is WMIP, (Wood’s Metal Intrusion Porosimetry) (Willis *et al.*, 1998). Based on the same principles, it additionally renders possible stabilizing the specimen through solidification of the used intrusion material. Hence, sections can thereupon be subjected to quantitative image analysis.

Quantitative image analysis is incidentally pursued for porosimetry (Scrivener, 1989; Lange *et al.*, 1994; Wang and Diamond, 1995; Hu and Stroeven, 2003), however the pore gradient structures resulting from the formation of the relatively porous Interfacial Transition Zones (ITZs) near the surfaces of the aggregate grains complicate the sampling operation; it thereby augments the time-consuming character of the analysis. In Hu (2004) and Stroeven *et al.* (2010) methods for 3D interpretation of 2D section images are reviewed, so the interested reader is referred to these publications focusing on experimental strategies to porosimetry.

Today it is readily possible economically producing realistic representations of the real-crete by means of advanced computer simulation methods. The pore network system developed after hydration simulation in the virtual computer-made concrete (“compcrete”) is thereupon available for quantitative geometrical and topological studies. Information like porosity, connected fraction of porosity, PoSD and pore tortuosity can be

obtained. This would permit representing the pore network structure by a tube system that incorporates the aforementioned information. Common hydraulic modelling strategies finally yield permeability information. This is demonstrated herein.

Unfortunately, most popular approaches in concrete technology produce compcrete by RSA (Random Sequential Addition) particle packing strategies, such as by  $\mu\text{ic}$  (Bishnoi and Scrivener, 2009) or by Hymostruc3D (Breugel, 1991). A modern porosimetry method developed by Ye (2003) for 3D reconstruction from serial sections of pore space in the hardened *virtual* cement paste is based on Hymostruc3D. Although it is basically possible directly deriving 3D information on PoSD from the virtual cementitious specimen, the results suffer from the deficiencies of RSA. This and other simulation methods including stochastic modelling approaches are discussed in Stroeven *et al.* (2010).

Two building blocks of a new modern methodology for porosimetry on virtual cementitious pastes - incorporating many stereological issues - were earlier published in IA&S (Stroeven *et al.*, 2012a,b). Since the pursued engineering information is basically of structure-sensitive nature, the packing of particles (aggregate and cement grains alike) should be conducted by DEM (Discrete Element Method) and not by either one of the in concrete technology popular RSA systems, since they produce virtual material with biased dispersion. As a consequence, fracture (He *et al.*, 2011) or durability estimates (see this publication) would be inevitably biased, too.

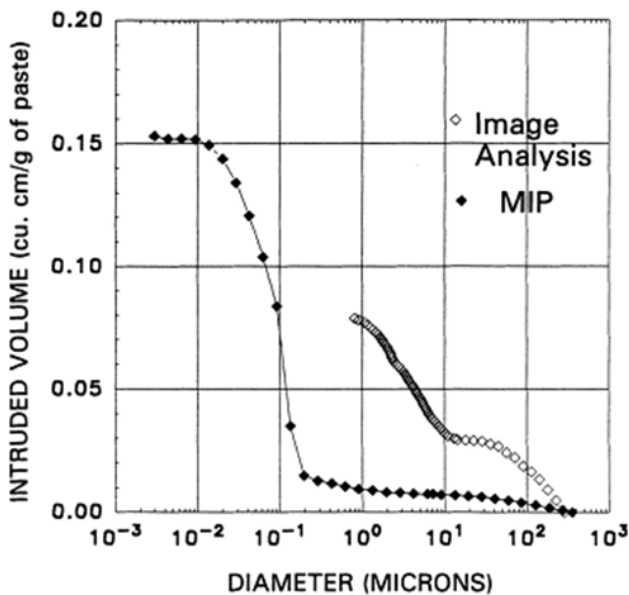


Fig. 1. Differences between porosimetry results obtained by image analysis and by MIP obtained on similar cementitious material samples (Diamond, 2000).

The dynamic force-based DEM system used in the presented research (Habanera's Discrete Element System, HADES) has already been described elsewhere (He, 2010; Stroeven *et al.*, 2011), so for details the reader is referred to these publications. The new vector-based (*i.e.*, geometric primitives-based) hydration simulation system, XIPKM, has also been published earlier (Le *et al.*, 2013). It is an extension of the well-known IPKM method commonly employed in producing *analogue* versions of the hardened material. See, *e.g.*, Navi and Pignat (2005). In alternative approaches, a digitized version of the material is produced and porosimetry is adapted to such a digitized set up. For representative studies, one is referred to work by NIST collaborators (*e.g.*, Garboczi and Bentz, 2001). Analogue approaches have however major advantages. Particularly, the scale sensitivity of the digitized approach constitutes a serious drawback. Moreover, uniform randomness (UR) in quite densely packed cement particle systems will not constitute a reliable representation of the realcrete. Hence, it was demonstrated earlier by Chen *et al.* (2006) that for similar cases, the pore depercolation *processes* during hardening were distinctly different for the DEM, RSA and digitized approaches.

So, the proposed strategy represents an analogue methodology for production of the material and of a quantitative assessment of pore network characteristics. It is readily available for application to engineering problems whereby durability constitutes a highly relevant issue. So far, all simulation systems assume cement grains to be spherical, the present one included. Recently, it was demonstrated however that real cement grains are more polyhedron-shaped (Garboczi and Bullard, 2004). This would complicate simulating particle interferences on micro-level in a hydrating system, however. Therefore, we are developing an algorithm for nano-level particle packing of the outer layer of calcium silicate hydrate (CSH) (Li *et al.*, 2014). This would render possible assuming cement particles to be poly-hedron-shaped. Moreover, surface roughness would be implemented on pore surfaces reducing conductance for water transport. This will be touched upon in the discussion section.

Of course, the permeability outcomes will be validated on the basis of available experimental data. Reliability of the various building blocks is validated in the various publications referred to. The internal moisture conditions of concrete thereby play a major role. This gives rise to partly saturated conditions in the pores that can lead to permeability data varying over three to four orders of magnitude. The controlling of this state is also a factor seriously hampering

the reliability of the outcomes of physical experiments that are potentially available for validation purposes.

## POROSIMETRY IN VIRTUAL CONCRETE

In general, five building blocks or stages of the proposed methodology can be distinguished. The first four are developed for *porosimetry* and will be briefly reviewed in what follows, since they are explicitly described in the international literature to which will be referred. Such publications also review other methods for porosimetry, *i.e.*, experimental studies, stochastic approaches and computer simulation methods, both DEM- as well as RSA-based. The successive building blocks are: particle packing by DEM, hydration simulation by XIPKM, pore delineation by DRaMuTS and pore measuring by SVM. The remaining block for permeability estimation will be discussed in the appropriate section.

### DEM-BASED PARTICLE PACKING

A dynamic force-based DEM denoted HADES is developed for packing simulation of basically artificially-shaped particles on meso-, micro- and nano-level. This is the first building block for porosimetry, but it was used as well on meso level for packing of non-spherical particles representing crushed rock aggregate (He, 2010). Application on micro-level, so far, involved spherical particles, because of the complications arising from interferences of hydrating non-spherical particles. We are presently exploring simulation of the outer CSH hydration layer on nano-level. This would, on the one hand, eliminate coping with interference problems by the vector (*i.e.*, geometry-based) approach. On the other hand, more realistic, polyhedron-types of particles could be considered (Garboczi and Bullard, 2004).

In the present case, the sequence of activities encompassed the following. As commonly done, a Rosin-Rammler function is specified to represent the particle size distribution of the Portland cement; *i.e.*,  $G(d) = 1 - \exp(-bd^a)$ , whereby  $G(d)$  stands for the mass or volume fraction of the cement passing a sieve with opening  $d$ , and  $a$  and  $b$  are constants (Hu, 2004). Mineral admixture particles will have their own grain size distribution.

The amount of cement and of the mineral admixture necessary to achieve the required water to binder ratio and blending percentage are assessed and the associated particles are dispersed by RSA procedure in an enlarged container, generally with two rigid and

four periodic boundaries (Fig. 2). The two opposite rigid boundaries are contrasted by green colour in this figure. This set up is selected to simulate the packing of the binder between neighbouring aggregate grain surfaces. Otherwise, six periodic boundaries are selected for simulating bulk material. Next, particles are set to linearly move and rotate according to Newtonian rules. When the afore-mentioned global state of particle density is reached, the dynamic stage is terminated. Note that global density can be as high as 0.6 (so close to random loose packing) for very low water to binder ratios applied in the (super) high performance range of concrete qualities.

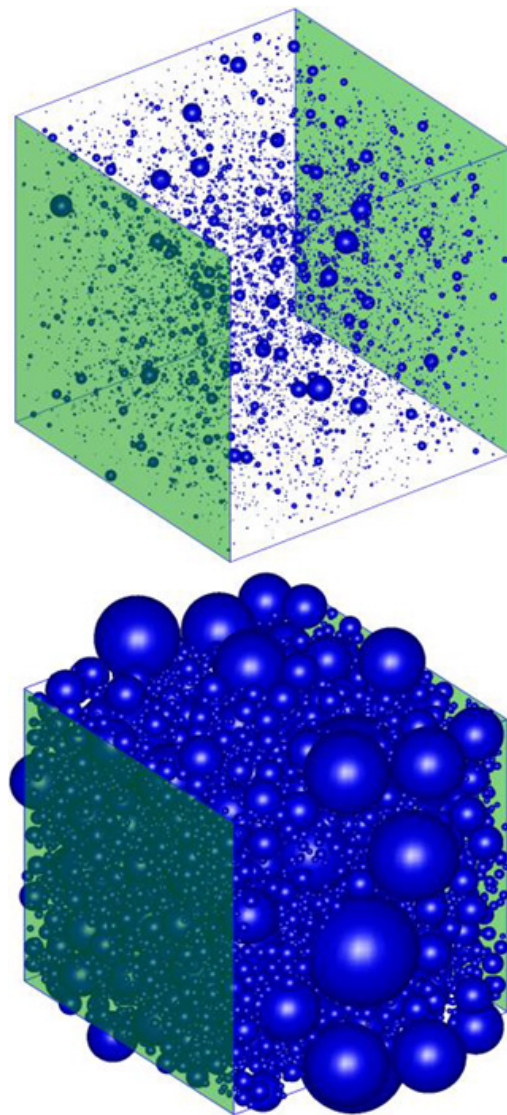


Fig. 2. Dilute dispersed particles in enlarged container at the top (initial stage) are densely packed at end of the dynamic stage (bottom picture). Green walls represent the rigid boundaries, while the rest are of the periodic type. For visualization purposes, the compacted container is shown on appropriately enlarged scale



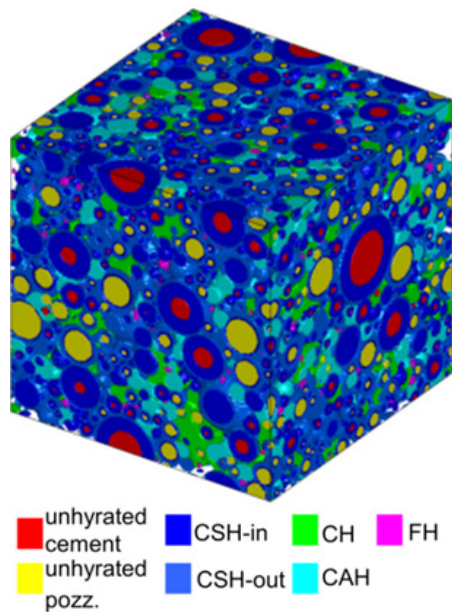


Fig. 5. 3D visualization of microstructure and corresponding pore space of a blended cement paste by a digital image based technique or voxel system. Each unhydrated multiphase core is represented by a sphere whose volume equals the total volume of the phases.

### PORE DELINEATION BY DRAMUTS

DRaMuTS, the third building block of the porosimetry methodology, stands for a Double Random Multiple Tree Structuring system for delineating the complete pore network and for topology assessment (Stroeven *et al.*, 2012a). By this method, randomized data structures are built incrementally in two stages. The first stage is to rapidly explore the pore space. Virtual trees consisting of nodes and lines connecting pairs of such nodes (like branches in real trees), grow randomly and incrementally in the pore medium. To speed up the process, deviating from the rapidly-exploring random tree approach, developed in robotics, a point is shifted to avoid rejections, thereby however violating the uniform randomness of the tree system. When neighbouring trees are developing in the same pore, they are forced to merge. In the second stage, a system of probing points is generated uniformly at random in pore space. As a result, such points can be used for statistical assessment of pore characteristics in which point classifications are realized by connections of such points to the tree systems. For example, the connected fraction of pores can be estimated by the fraction of the total number of points that can be associated with the percolated tree branches. Fig. 6 presents the pore network structure as obtained by DRaMuTS. At the top all pore trees are displayed, at the bottom only those connecting outer surfaces of the simulated specimen (the so called main trunks).

Note that different colours in Fig. 6 (top) represent the various trees growing from different seeds. These seeds can be generated on both top and bottom surfaces of the cube to speed up the calculation. The pores that are delineated by zigzag lines are smoothed by mathematical operations so that they can be used for permeability estimation by a network model.

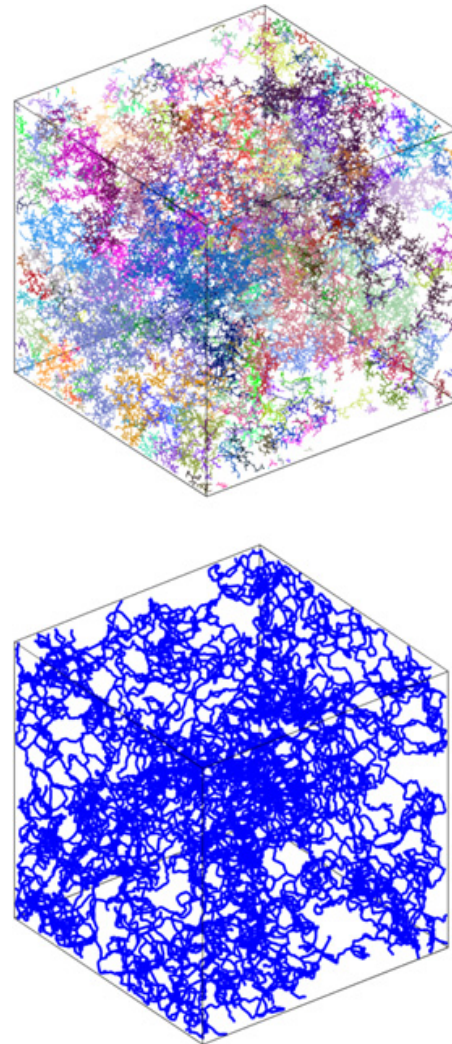


Fig. 6. Pore delineation in 100µm cubes for a plain PC sample. The various trees are characterized by different colors. All trees growing in capillary pores are shown (top) as well as the extracted main trunks only (bottom).

### PORE GEOMETRY AND TOPOLOGY

Topology of the pore network structure is already assessed on the basis of the tree morphology. Thereupon, star volume measuring (SVM) in UR dispersed points inside the pore network is applied (Stroeven *et al.*, 2010). This is the fourth building block for porosimetry. The PoSD is obtained from SVM whereby the UR points are employed as the nuclei of “stars”. In each point a system of pikes is generated



The flow inside a *tube* with constant circular cross section is assumed to be slow, saturated, incompressible and laminar according to the Hagen-Poiseuille law. The irregular *shapes* of the pore cross-sections are still taken into account in estimating the hydraulic conductance of the tubes. Fig. 8 shows the “inefficiency” of a randomly selected cross-sectional shape for transport (Le, 2015).

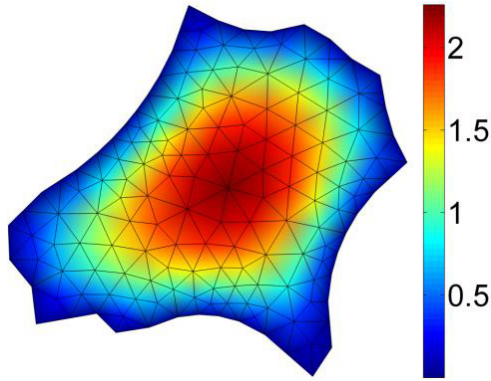


Fig. 8. Relative information on the velocity field of water flow through an irregular cross-section of a pore solved by FEM.

For an ideal circular cross-section, the conductance  $C$  can be derived from the Hagen–Poiseuille's equation and expressed by:

$$C_{cir} = \frac{\pi D^4}{128\mu}, \quad (2)$$

where  $D$  is the diameter of the circular section. In the section, the flow distribution is parabolic. However, the cross-sections of capillary pores in cementitious porous media are generally as irregularly-shaped as depicted by Fig. 8. The influence of the shape factor should therefore be taken into account for the estimation of cross-sectional conductance. Patzek and Silin (2001) investigated conductance of non-circular cross-sections, *i.e.*, triangular, rectangular and elliptic shapes, in which the cross-sectional conductance is shown to be proportional to the shape factor of the cross-section. The shape factor in such investigations is expressed through the dimensionless ‘shape factor’  $Sh$  of Mason and Morrow (1991)

$$Sh = \frac{A}{P^2}, \quad (3)$$

where  $A$  and  $P$  denote the cross-sectional area and the perimeter length, respectively. Note that this is inversely proportional to *circularity* used in concrete technology (Hu and Stroeven, 2006; Stroeven *et al.*, 2009; He, 2010).

The velocity is integrated over the cross-sectional area to obtain the volumetric rate and therefore the hydraulic conductance. Fig. 8 is an example of the velocity field of a cross-section of a pore in a simulated cement paste; the geometrical configuration of the pore section is obtained by the enhanced SVM (Le, 2015). This involves a shift in the location of the random node in the throat section to that of the nucleus of the representative circle. Fig. 9 shows the relation between dimensionless conductance of pore sections (pore throats) in a matured (*i.e.*, hardened) cement specimen and their dimensionless shape factors, in comparison to such relations for random triangles and quadrilaterals. Obviously, all values of conductance as well as shape factor  $Sh$  are smaller than those of the circular section, *i.e.*,  $\tilde{C}_{cir} = 1/8\pi \approx 0.04$  and  $Sh_{cir} = 1/4\pi \approx 0.08$ .

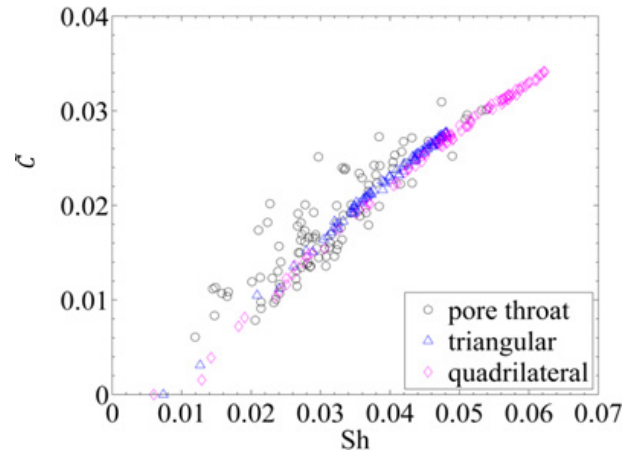


Fig. 9. Dimensionless hydraulic conductance versus shape factor for 100 pore cross-sections (throats) of a simulated cement paste; 100 random triangles and 100 random quadrilaterals.

To obtain the conductance of all equivalent tubes, the cross-sectional hydraulic conductance can be calculated at the pore throats along the main trunks. However, solving the flow by FEM at every pore throat would be not practical. In this study, hence, the influence of the shape factor on conductance is integrated statistically; the dimensionless conductance is estimated by FEM at an adequate number of random points in pore space. The obtained values are then used to form a function yielding the conductance for arbitrary pore throats via its shape factor. For example, the conductance versus shape factor of pore throats is shown (in relative terms with respect to a circular section) and fitted by a linear function as in Fig. 10. Herein, the hydraulic conductance of a pore throat is given by

$$\tilde{C}_{po} = \tilde{C}_{cir}\zeta, \quad (4)$$



practice. Muller *et al.* (2013) recently showed by  $^1\text{H}$  NMR relaxation analysis that for a white cement paste with a water-cement-ratio of 0.4, the total capillary porosity was 9.2% by volume after 28 days of hydration; only 1.4% was filled by unconsumed water and the rest were ‘empty’ chemical shrinkage voids. They further found it difficult (if not impossible) to subsequently refill these voids (Zalzal *et al.*, 2013).

To model permeability at various degrees of water saturation, an “emptying” algorithm was implemented. In this algorithm, water was removed progressively

by evaporation from fully saturated microstructures, starting from the largest pores according to the Kelvin-Laplace law, following Zalzal *et al.* (2013). The positions and diameters of pores were determined using DRaMuTS and SVM. Next, all pores were sorted by their sizes and stored for further analysis. In this way, it is easy to find the largest pores. Once their positions were determined, some virtual spheres with the same sizes as the corresponding pores could be placed to block the original transport path for water, representing the partially saturated state, as illustrated in Fig. 12.

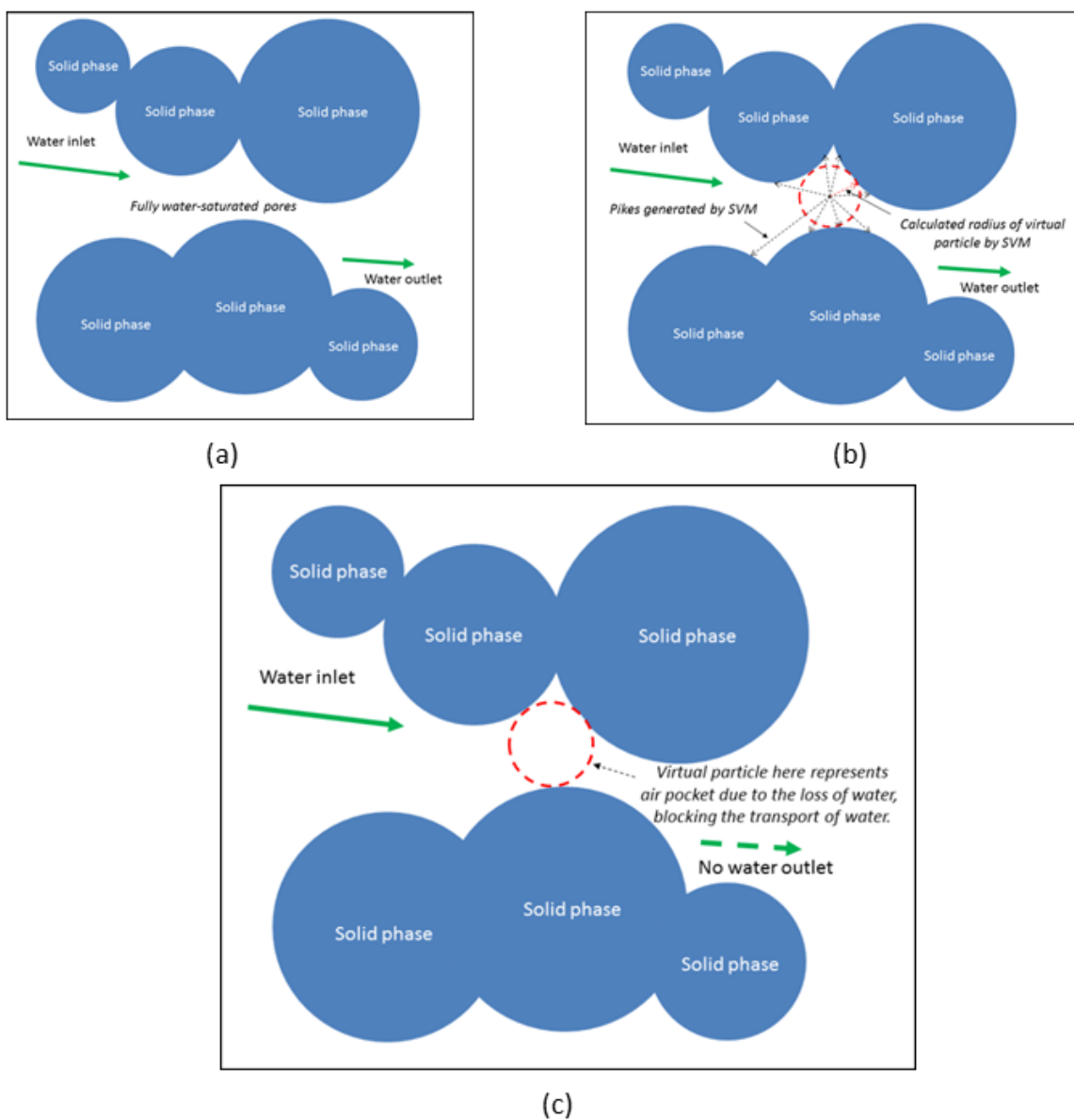


Fig. 12. Illustration of the “emptying” algorithm in 2D: (a) Fully saturated state; (b) assessment of smallest pore for positioning of a solid disc in water-filled pore. (c) Partially saturated state. The position and size of the solid disc (red circle) are obtained by DRaMuTS.



of points. A large number of points usually leads to more accurate results, but yields excessive computational efforts and time. Therefore, a sensitivity analysis of connected pore fraction at various degrees of water saturation was carried out. The results are plotted in Fig. 15.

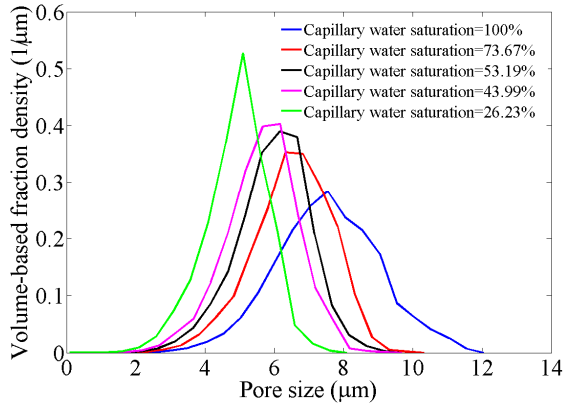


Fig. 13. Pore size distribution of samples at various degrees of water saturation.

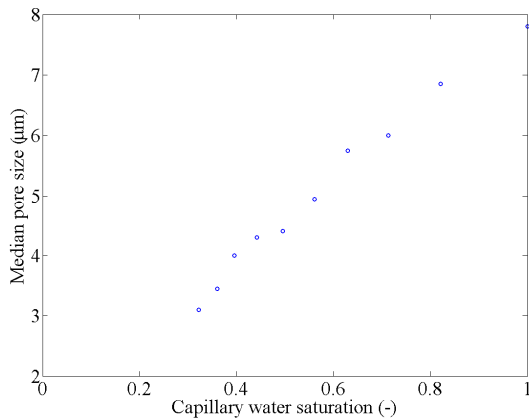


Fig. 14. Almost linear reduction in median pore size with declining degree of water saturation in the capillary pore network structure.

Obviously, connected pore fraction increases sharply as the number of points goes up, where-upon the curves bend to reach a plateau level. In the present research,  $10^5$  points are used in all cases to minimize computation time in combination with a high accuracy level. Connected pore fraction is plotted as a function of capillary water saturation in Fig. 16. With decreasing capillary water saturation, the fully water-filled pores will gradually become blocked by air bubbles, leading to a reduced connected pore fraction of the microstructures. This rate of decline increases at further reduction of the degree of saturation, as a direct reflection of the increased spacing of the curves in Fig. 15.

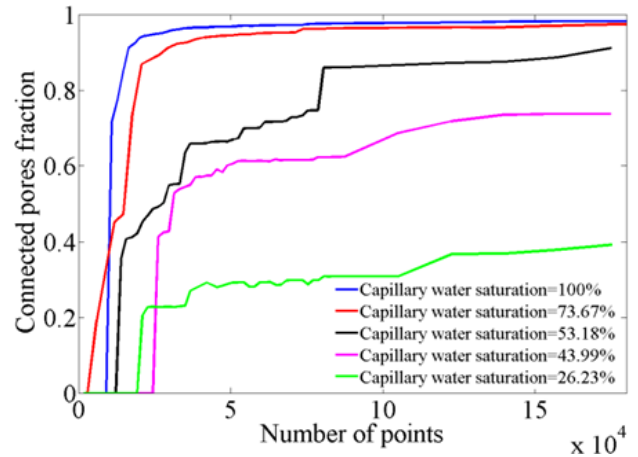


Fig. 15. Sensitivity analysis of connected pore fraction at various degrees of water saturation.

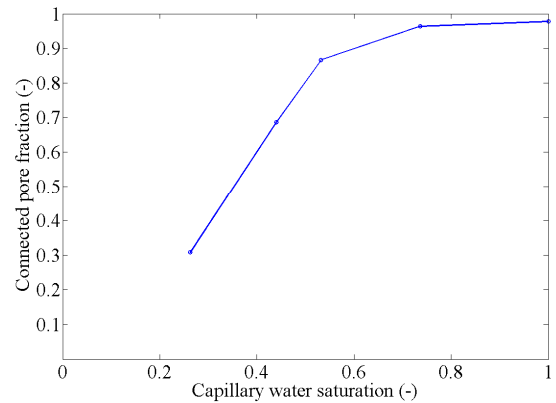


Fig. 16. Connected pore fraction as a function of capillary water saturation.

## VALIDATION

To compare with the available experimental data obtained on *concrete*, relative permeability is plotted in Fig. 17. This is defined as the ratio of intrinsic permeability at a certain degree of saturation to intrinsic permeability measured in the fully saturated state. In the case of water permeability, a sample fully filled by water implies that the water saturation equals 1. Obviously, an agreement between experimental data and simulation results obtained by the presented methodology is very satisfactory, validating the presented methodological approach.

It should be noted again that the extreme values of water saturation were most probably not realized in the reported experiments shifting the associated curves even more closer to the simulation results. Of course, Fig. 17 reveals the joint effects of the two discussed parameters, PoSD and connectivity.



The methodology is presently exploited for systematically investigating effects of technological and environmental parameters on durability capacity (when based, of course, on transport through the capillary pores). The relevant results of such technological studies will be published elsewhere.

## REFERENCES

- Abbas A, Carcasses M, Ollivier JP (1999). Gas permeability of concrete in relation to its degree of saturation. *Mater Struct* 32:3–8.
- Abell AB, Willis KL, Lange DA (1999). Mercury intrusion porosimetry and image analysis of cement-based materials. *J Colloid Interf Sci* 211:39–44.
- Bamforth PB (1987). The relationship between permeability coefficients for concrete obtained using liquid and gas. *Mag Concr Res* 39:3–11.
- Banthia N, Mindess S (1989). Water permeability of cement paste. *Cem Concr Res* 19:727–36.
- Baroghel-Bouny V, Thiery M, Wang X (2011). Modelling of isothermal coupled moisture-ion transport in cementitious materials. *Cem Concr Res* 41:828–41.
- Chen H, Stroeven P, Ye G, Stroeven M (2006). Influence of boundary conditions on pore percolation in model cement paste. *Key Eng Mat* 302–303:486–92.
- Chiu SN, Stoyan D, Kendall WS, Mecke J (2013). *Stochastic geometry and its applications*, 3rd Ed. Chichester: Wiley.
- Coussy O, Eymard R, Lassabatere T (1998). Constitutive unsaturated modeling of drying deformable materials. *J Eng Mech* 124:658–67.
- Diamond S (2000). Mercury porosimetry: an inappropriate method for the measurement of pore size distribution in cement-based materials. *Cem Concr Res* 30:1517–25.
- Dhir RK, Hewlett PC, Chan YN (1989). Near surface characteristics of concrete: intrinsic permeability. *Mag Concr Res* 41:87–97.
- Garboczi EJ, Bentz, DP (2001). The effect of statistical fluctuation, finite size error, and digital resolution on the phase percolation and transport properties of the NIST cement hydration model. *Cem Concr Res* 31:1501–14.
- Garboczi EJ, Bullard JW (2004). Shape analysis of a reference cement. *Cem Concr Res* 34:1933–7.
- Gundersen HJG, Bendtsen TF, Korbo L, Marcussen N, Møller A, Nielsen K, *et al.* (1988). Some new, simple and efficient stereological methods and their use in pathological research and diagnosis. *APMIS* 96:379–94.
- He H (2010). Computational modelling of particle packing in concrete. PhD Thesis, Delft University of Technology. Delft.
- He H, Stroeven P, Stroeven M and Sluys LJ. (2011). Influence of particle packing on fracture properties of concrete. *Comp Concr* 8:677–92.
- Hearn N, Detwiler RJ, Sframeli C (1994). Water permeability and microstructure of three old concretes. *Cem Concr Res* 24:633–40.
- Hu J, Stroeven P (2003). Application of image analysis to assessing critical pore size for permeability prediction on cement paste. *Image Anal Stereol* 22: 7–103.
- Hu J (2004). Porosity of concrete: Morphological study of model concrete. PhD Thesis, Delft University of Technology. Delft.
- Hu J, Stroeven P (2006). Shape characterization of concrete aggregate. *Image Anal Stereol* 25:43–53.
- Kameche ZA, Ghomari F, Choinska M, Khelidj A (2014). Assessment of liquid water and gas permeabilities of partially saturated ordinary concrete. *Construct Build Mater* 65:551–65.
- Lange DA, Jennings HM, Shah SP (1994). Image analysis techniques for characterization of pore structure of cement-based materials. *Cem Concr Res* 24:841–53.
- LaValle SM and Kuffner JJ (2001). Rapidly-exploring random trees: progress and prospects. In: Donald BR, Lynch KM and Rus D, eds. *Algorithmic and computational robotics: New directions*. Wellesley (Ma).
- Le LBN (2015). Micro-level porosimetry of virtual cementitious materials – Structural impact on mechanical and durability evolution. PhD Thesis, Delft University of Technology. Delft.
- Le LBN and Stroeven P (2014). Packing issue in cement blending for sustainability developments – Approach by discrete element method. *Int J Res Eng Technol* 3:89–96.
- Le LBN, Stroeven M, Sluys LJ, Stroeven P (2013). A novel numerical multi-component model for simulating hydration of cement. *Comp Mater Sci* 78:12–21.
- Le LBN, Stroeven P (2012). Porosity of green concrete based on a gap-graded blend. In: Brandt AM, Olek MA and Leung CKY, eds. *Proceedings of the International Symposium on Brittle Matrix Composites 10*, 2012 October 15–17; Warsaw, Poland, 315–24.
- Li K, Le LBN, Stroeven P, Stroeven M (2014). Strategy for predicting transport-based durability properties of concrete based on DEM approach. In: Bjegovic D, Beushausen H, Serdar M, eds. *Proceedings of the RILEM International Workshop on Performance-based Specification and Control of Concrete Durability*, 2014 June 11–13; Zagreb, Croatia, 443–50.
- Loosveldt H, Lafhaj Z, Skoczylas F (2002). Experimental study of gas and liquid permeability of a mortar. *Cem Concr Res* 32:1357–63.
- Mason G and Morrow NR (1991). Capillary behaviour of a perfectly wetting liquid in irregular triangular tubes. *J Colloid Interf Sci* 141:262–74.
- Muller ACA, Scrivener KL, Gajewicz AM, McDonnald PJ (2013). Densification of C-S-H measured by <sup>1</sup>H NMR relaxometry. *J Phys Chem C* 117:403–12.

- Patzek TW, Silin DB (2001). Shape factor and hydraulic conductance in noncircular capillaries: One-phase creeping flow. *J Colloid Interf Sci* 236:295-304.
- Pignat C, Navi P, Scrivener K (2005). Simulation of cement paste microstructure, hydration, pore space characterization and permeability determination. *Mat Struct* 38: 450–66.
- Richardson IG (2004). Tobermorite/jennite- and tobermorite/calcium hydroxide-based models for the structure of C-S-H: Applicability to hardened pastes of tricalcium silicate,  $\beta$ -dicalcium silicate, Portland cement, and blends of Portland cement with blast-furnace slag, metakaolin, or silica fume. *Cem Concr Res* 34:1733–77.
- Scrivener KL (1989). The use of backscattered electron microscopy and image analysis to study the porosity of cement paste. In: Roberts LR, Skalny JP, eds. *Proceedings of material research society symposium 137*, 1989; Warrendale, PA, 129–40.
- Stroeve P, Hu J, Guo Z (2009). Shape assessment of particles in concrete technology: 2D image analysis and 3D stereological extrapolation. *Cem Concr Compos* 31: 84–91.
- Stroeve P, Hu J, Koleva DA (2010). Concrete porosimetry: Aspects of feasibility, reliability and economy. *Cem Concr Compos* 32:291–99.
- Stroeve P, He H, Stroeve M (2011). Discrete element approach to assessment of granular properties in concrete. *J Zhejiang Univ – Sci A* 12:335–44.
- Stroeve P, Le LBN, Sluys LJ, He H (2012a). Porosimetry by double random multiple tree structuring. *Image Anal Stereol* 31:55–63.
- Stroeve P, Le LBN, Sluys LJ, He H (2012b). Porosimetry by random node structuring in virtual concrete. *Image Anal Stereol* 31:79–87.
- Stroeve P, Le LBN (2013). Evaluation by discrete element method (DEM) of gap-graded packing potentialities for green concrete design. In: Soustos M, Goodier C, Nguyen VT, eds. *The International Conference on Sustainable Built Environment for Now and the Future*, 2013 March 26–27; Hanoi, Vietnam, 347–54.
- Vogel HJ and Roth K (2001). Quantitative morphology and network representation of soil pore structure. *Adv Water Resour* 24:233–44.
- Wang Y, Diamond S (1995). An approach to quantitative image analysis for cement pastes. In: Diamond S, Mindess S, Glasser FP, Roberts LW, Skalny JP, Wakeley LD, eds. *Microstructure of cement based systems/ bonding and interfaces in cementitious materials*, Vol. 370 Material Research Society, Pittsburgh, 23–32.
- Willis KL, Abell AB and Lange DA. (1998). Image-based characterization of cement pore structure using wood's metal intrusion. *Cem Concr Res* 28:1675–1705.
- Williams SR and Philipse AP (2003). Random packings of spheres and spherocylinders simulated by mechanical contraction. *Phys Rev E* 67:1–9.
- Wong H, Buenfeld N, Hill J, Harris A (2007). Mass transport properties of mature wasteform grouts. *Adv Cem Res* 19:35–46.
- Wong HS, Zobel M, Buenfeld NR, Zimmerman RW (2009). Influence of the interfacial transition zone and microcracking on the diffusivity, permeability and sorptivity of cement-based materials after drying. *Mag Concr Res* 61:571–89.
- Ye G (2003). Experimental study and numerical simulation of the development of the microstructure and permeability of cementitious materials. PhD Thesis, Delft University of Technology. Delft.
- Zalzale M, McDonnald PJ, Scrivener KL (2013). A 3D lattice Boltzmann effective media study: understanding the role of C-S-H and water saturation on the permeability of cement paste. *Modelling Simul Mater Sci Eng* 21:085016.